



ACADEMIC  
PRESS

Available online at [www.sciencedirect.com](http://www.sciencedirect.com)

SCIENCE @ DIRECT®

Journal of Solid State Chemistry 177 (2004) 221–226

JOURNAL OF  
SOLID STATE  
CHEMISTRY

<http://elsevier.com/locate/jssc>

# Mechanical alloying of a thermoelectric alloy: $\text{Pb}_{0.65}\text{Sn}_{0.35}\text{Te}$

N. Bouad, M.-C. Record, J.-C. Tedenac, and R.-M. Marin-Ayral\*

*Laboratoire de Physico-chimie de la Matière Condensée, Université Montpellier II, CC003, Pl. E. Bataillon, 34095 Montpellier, Cedex 5, France*

Received 12 April 2003; received in revised form 22 July 2003; accepted 23 July 2003

## Abstract

We report in this paper a study of the mechanical alloying (MA) process for the  $\text{Pb}_{0.65}\text{Sn}_{0.35}\text{Te}$  alloy. MA has been carried out in a high-energy planetary ball mill. The mechanism of formation has been studied from systematic analyses of mechanically alloyed powders using X-ray diffraction, differential scanning calorimetry and scanning electron microscopy. As it was already observed for the MA of PbTe, this synthesis is associated with an exothermic reaction between the elemental powders. The required time to reach an homogeneous phase  $\text{Pb}_{0.65}\text{Sn}_{0.35}\text{Te}$  is 31 h.

© 2003 Elsevier Inc. All rights reserved.

*Keywords:* Mechanical alloying; X-ray diffraction; Thermal analyses; Thermoelectricity

## 1. Introduction

PbTe and its related alloys (mostly  $\text{Pb}_{1-x}\text{Sn}_x\text{Te}$ ) are well known as thermoelectric materials for middle range temperature applications (500–700 K) [1,2]. The PbTe–SnTe system which is a quasi-binary one, shows a complete solid solution [3], thus single-phase materials can be obtained from pure PbTe to pure SnTe. Thermoelectric measurements have been carried out on these alloys by many authors [2,4–9]. The performance of a thermoelectric material is usually expressed by the figure of merit  $Z$  represented by  $Z = S^2\sigma/\kappa$ , where  $S$  is the Seebeck coefficient,  $\sigma$  the electrical conductivity and  $\kappa$  the thermal conductivity [10]. The Seebeck coefficient decreases from PbTe to SnTe and for each composition it shows a maximum with relation to temperature. When the tin content increases, this maximum value is shifted to a higher temperature [9]. The highest figure of merit ( $Z = 1.2 \times 10^{-3} \text{K}^{-1}$ ) was observed for the  $\text{Pb}_{0.7}\text{Sn}_{0.3}\text{Te}$  alloy at 350 K [4]. Thus, in order to obtain good thermoelectric characteristics for applications around 500 K, the  $\text{Pb}_{0.65}\text{Sn}_{0.35}\text{Te}$  alloy was chosen for the preparation.

The conventional method used in the industrial production of thermoelectric powders (vacuum melting, chill cooling and grinding) requires long processing time, high temperature and large scale facilities which

are costly, therefore, industrials are looking for cost-saving processes. As mechanical alloying (MA) occurs near room temperature, it could be one of the processes, as it has already been reported successfully in previous literature [11–15].

MA is performed in high-energy ball mills and produces solid solutions by means of repeated mechanical impacts. The features of the MA process are the formation of uniform elemental dispersion and small powder particle size. As the propagation of charge carriers and phonons is affected by the geometrical limits of the crystallites and as the thermal conductivity at 500–700 K is dominated by the lattice contribution, the figure of merit is expected to be enhanced when homogeneous low crystallite sizes are achieved. Thus, MA seems to be a very promising process for thermoelectric powder production.

In a previous publication [15], we reported the successful synthesis of PbTe by MA and the study of this process using X-ray diffraction (XRD), differential scanning calorimetry (DSC) and scanning electron microscopy (SEM). In the present paper, we provide results of a similar study on  $\text{Pb}_{0.65}\text{Sn}_{0.35}\text{Te}$  alloy.

## 2. Experimental procedure

MA was carried out in a planetary mill (Fristch® Pulverisette P7) operating at 596 rpm which was stopped every hour for a period of 30 min in order to prevent

\*Corresponding author. Fax: +33-04-67144290.

E-mail address: [ayral@lpmc.univ-montp2.fr](mailto:ayral@lpmc.univ-montp2.fr) (R.-M. Marin-Ayral).

hasty engine wear. Loading, milling and unloading were made under an argon atmosphere to prevent oxidation of the powders. Granules of lead (99.9995%), tin (99.95%) and tellurium (99.999%) with a diameter of 3 mm were weighed according to the stoichiometry of  $\text{Pb}_{0.65}\text{Sn}_{0.35}\text{Te}$  and introduced in a 45 mL  $\text{Si}_3\text{N}_4$  vial with  $\text{Si}_3\text{N}_4$  balls. The material to ball weight ratio was kept constant at 1:2 for every synthesis. The milling was performed at different times: 1 h, 3 h, 6 h, 12 h, 31 h, and after each reaction time, the powder was analyzed by means of XRD, DSC and SEM. It is important to mention that these syntheses are independent. Indeed, for short milling times when the reaction is not complete, a deduction of powder would modify the composition of the batch for upcoming steps.

XRD measurements were carried out on a  $\theta$ - $2\theta$  X-ray diffractometer equipped with a monochromator. Data acquisition was done for  $20 < 2\theta < 120^\circ$  with a step size of 0.02 and a step time of 9 s.

DSC was performed with a heat flow apparatus calorimeter, which has the following characteristics: a temperature range from 153 to 1103 K and a sensitivity limit of detection from 5 to 15 mV. In order to protect the samples from oxidation, these experiments were done in sealed quartz ampoule under vacuum. The heating rate was 5 K/min.

SEM coupled with energy dispersive X-ray analyses (EDX) was used to examine the milled powders and determine their atomic composition.

### 3. Results and discussion

#### 3.1. XRD analyses

Fig. 1 shows a sequence of XRD patterns of milled powders after different reaction times: 1 h, 3 h, 6 h, 12 h and 31 h.

For the first stages of milling, peaks corresponding to the pure elements are still observed. They disappear after 6 h for lead, 12 h for tin and 31 h for tellurium. In our previous study concerning MA of PbTe, tellurium was less persistent [15].

Peaks corresponding to the  $\text{Pb}_{1-x}\text{Sn}_x\text{Te}$  solid solution always appear on these patterns, even after the first hour of milling, but in the latter case these peaks seem to correspond to multiple ones, specially for the (200) and (220). This could be due to the coexistence of the same phase  $\text{Pb}_{1-x}\text{Sn}_x\text{Te}$  with different contents in tin which can be deduced from the angular values. The major one corresponds to the maximum of intensity, when milling time increases, these maxima are shifted towards the large angles. Taking into account these values, the lattice parameter was calculated and the composition deduced using the evolution reported by Tao and Wang [16]. Results are listed in Table 1.

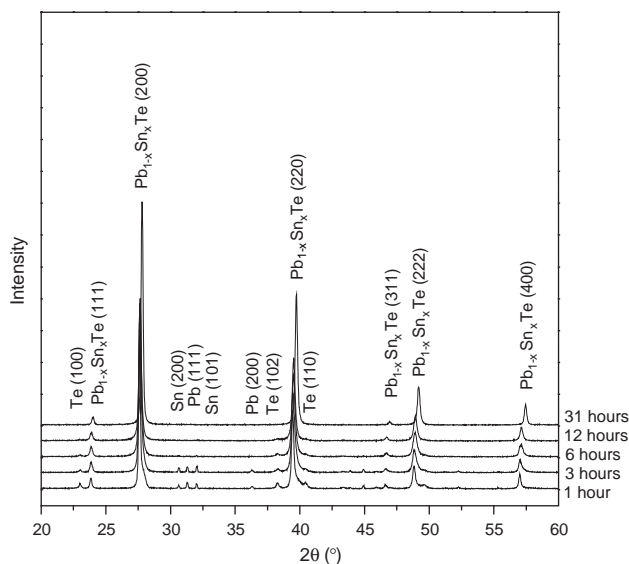


Fig. 1. X-ray diffraction patterns of Pb-Sn-Te powders for different times of milling.

Before reaching the nominal value, the synthesis proceeds in stages. A first level is observed at around 2%, and second one around 10%. After 31 h of milling, XRD results lead us to conclude that the elaboration of pure  $\text{Pb}_{0.65}\text{Sn}_{0.35}\text{Te}$  alloy is accomplished.

#### 3.2. Scanning electron microscopy

For the first stages of milling, several phases with different morphologies and compositions were identified by means of SEM (Fig. 2).

As it was already evidenced for the PbTe MA powders [15], two kinds of microstructures were observed: a cellular one (Fig. 2a and b), and a laminar one (Fig. 2c).

Table 2 gives the composition of the different phases numbered from 1 to 7 in Fig. 2.

In agreement with XRD and DSC results, pure tin, pure tellurium and  $\text{Pb}_{1-x}\text{Sn}_x\text{Te}$  with different compositions were evidenced. In contrast, pure lead was not found.

The cellular structures, similar to those generated by a liquid phase sintering [17], suggest the appearance of a melted phase during the milling process. However, the heat generated from the kinetic energy of the milling media is not enough to melt these powders, thus an exothermic reaction must occur locally. Morphology of the grains seems to depend on the generated liquid: spheroid with liquid Te (Fig. 2a) or faceted with liquid Sn (Fig. 2b).

In the laminar structure, powders are welded by a mechanism of diffusion.

After 31 h of milling, the powder is homogeneous, it consists of spherical agglomerates (Fig. 3) with very close compositions. EDX measurements were performed

Table 1  
Lattice parameters of  $\text{Pb}_{1-x}\text{Sn}_x\text{Te}$  for different milling times and approximate tin content from Tao and Wang's study [16]

Milling time (hours)	1	3	6	12	31
Lattice parameter ( $\text{\AA}$ )	$6.4565 \pm 0.0007$	$6.457 \pm 0.002$	$6.442 \pm 0.002$	$6.4460 \pm 0.0008$	$6.4113 \pm 0.0004$
Tin content in $\text{Pb}_{1-x}\text{Sn}_x\text{Te}$ (at%)	2.6	2.2	13.5	10.5	36.6

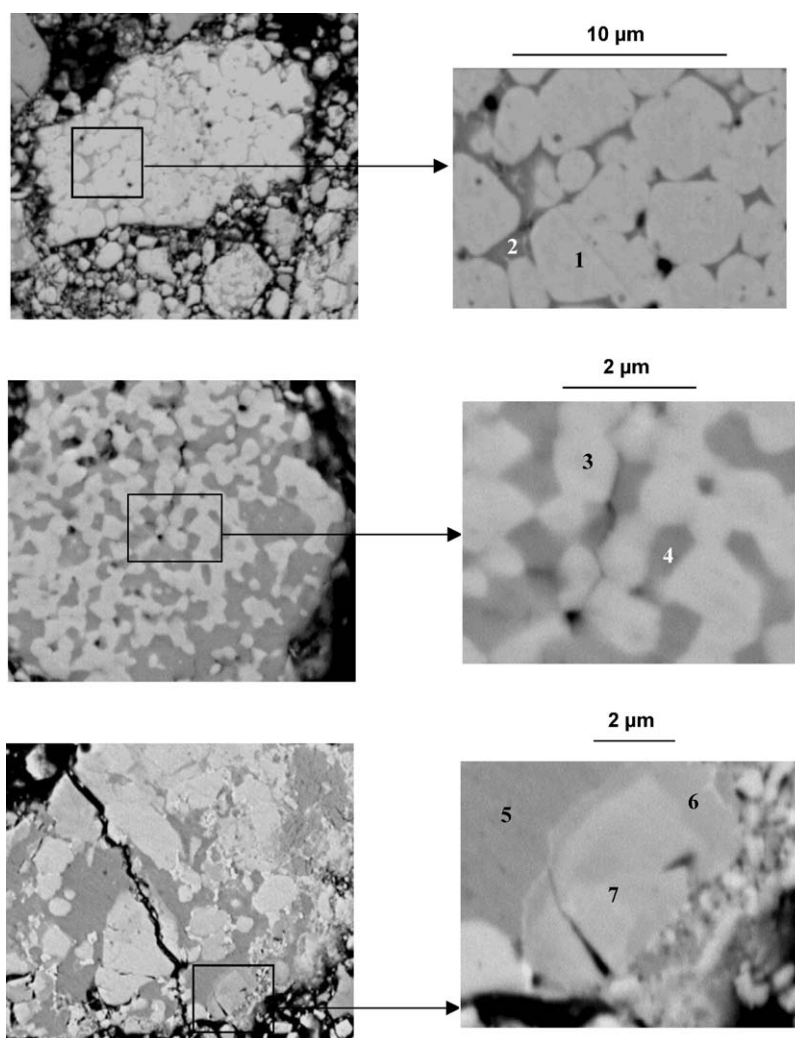


Fig. 2. SEM micrographs of MA powders after 1 h of milling, several phases have been characterized.

Table 2  
Composition of the phases observed for 1 h milled powder. Phase numbering is given in Fig. 2

Phase number	1	2	3	4	5	6	7
at% Pb	48	0	47	0	0	14	23
at% Sn	2	0	3	100	100	36	27
at% Te	50	100	50	0	0	50	50

on this sample in several places and only three different compositions ( $\text{Pb}_{0.64}\text{Sn}_{0.38}\text{Te}_{0.98}$ ,  $\text{Pb}_{0.66}\text{Sn}_{0.36}\text{Te}_{0.98}$ ,  $\text{Pb}_{0.66}\text{Sn}_{0.37}\text{Te}_{0.97}$ ) were found, they are in accordance with the nominal composition.

### 3.3. Differential scanning calorimetry

Thermograms recorded on heating for  $\text{Pb}_{1-x}\text{Sn}_x\text{Te}$  milled powders after different reaction times are reported in Fig. 4. Two cycles were made on each sample.

Below the endothermic effect at 680 K which exists on all the thermograms, three thermal effects are observed. The first one, endothermic, at 456 K solely exists for a milling time of 1 h, the second one, also endothermic, at 490 K disappears after 6 h of milling and the third one, exothermic and wider, is present for 1, 3 and 31 h of milling.

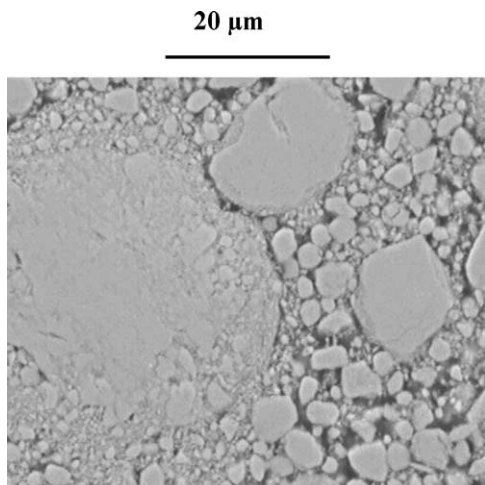


Fig. 3. SEM of  $\text{Pb}_{0.65}\text{Sn}_{0.35}\text{Te}$  MA powder after 31 h of milling.

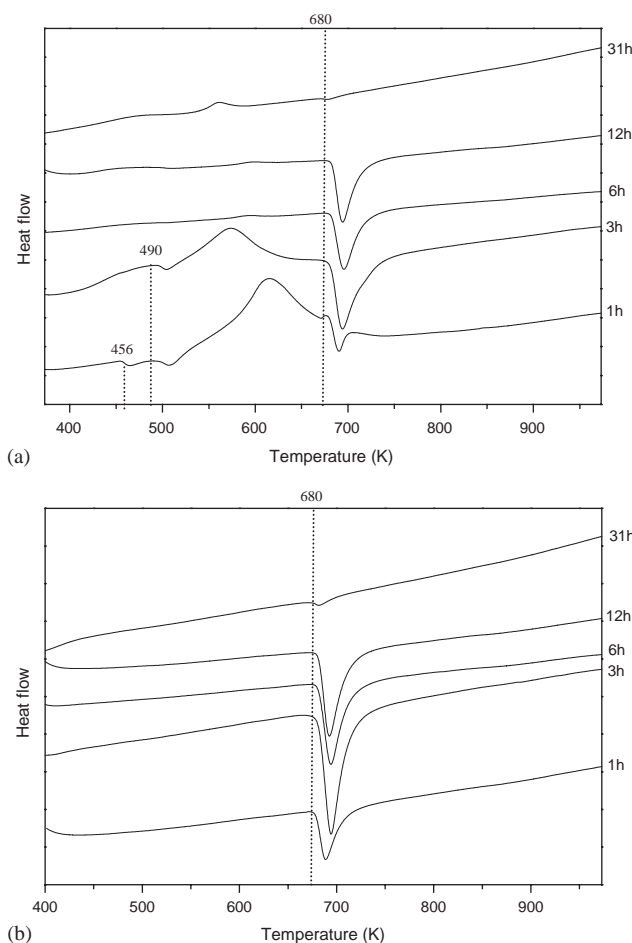


Fig. 4. Thermograms of  $\text{Pb-Sn-Te}$  powders recorded after different times of milling. (a) Heating part of the first cycles and (b) heating part of the second cycles.

On the second cycle recordings, whatever the time of milling, the only remaining effect is the endothermic one at 680 K.

Because of the presence of several phases in the first stages of milling, origin of these thermal effects can be found in a large domain of the  $\text{Pb-Sn-Te}$  phase diagram. Thus, the  $\text{Sn}_{35}\text{Pb}_{65}\text{-Te}$  section which crosses all the multi-phase field of this ternary requires consideration. This section calculated with Thermocalc from Kattner's results [18] is plotted in Fig. 5. As it was expected, the observed endothermic thermal effects correspond to phase transformations. Numbers 1–3 indicate the observed reactions. In agreement with the X-ray diffractograms, these results show for the first hours of milling, the coexistence of phases belonging to the  $[(\text{Sn})+(\text{Pb})+(\text{Sn,Pb})\text{Te}]$ ,  $[\text{Sn}+(\text{Sn,Pb})\text{Te}]$  and  $[(\text{Sn,Pb})\text{Te}+\text{Te}]$  fields.

Further transformations around 500 K (4) and 700 K (5) should be observed, but the presence of more energetic effects at related temperatures hides them.

The small thermal effect observed after 31 h of milling for a temperature slightly lower than 680 K can also be explained taking into account the  $\text{Sn}_{35}\text{Pb}_{65}\text{-Te}$  section. A zoom of its central part is given in Fig. 6 and heating of this sample is represented by the dotted line.

The observed thermal effect corresponds to the crossing between the  $[(\text{Sn,Pb})\text{Te}+\text{Te}]$  field and the  $(\text{Sn,Pb})\text{Te}$  one. It indicates the presence in this powder of a very small quantity of tellurium (less than 0.1 at%) which could not be evidenced by X-ray measurements.

As only one endothermic effect at 680 K appears on second heating cycles, the exothermic phenomena could be due to reactions, induced by temperature rise, between lead, tin and tellurium, at least for the first hours of milling. The conglomerates observed after interrupting the heating at 650 K tend to support this

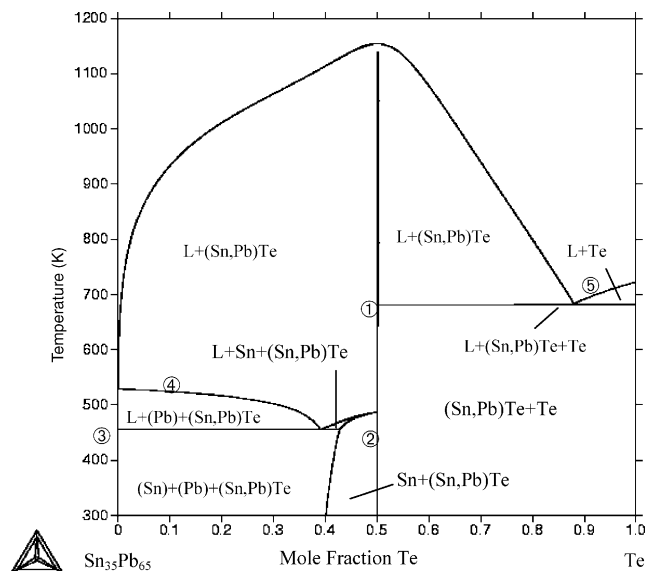


Fig. 5. The  $\text{Sn}_{35}\text{Pb}_{65}\text{-Te}$  section calculated using Thermocalc program from Kattner's results.

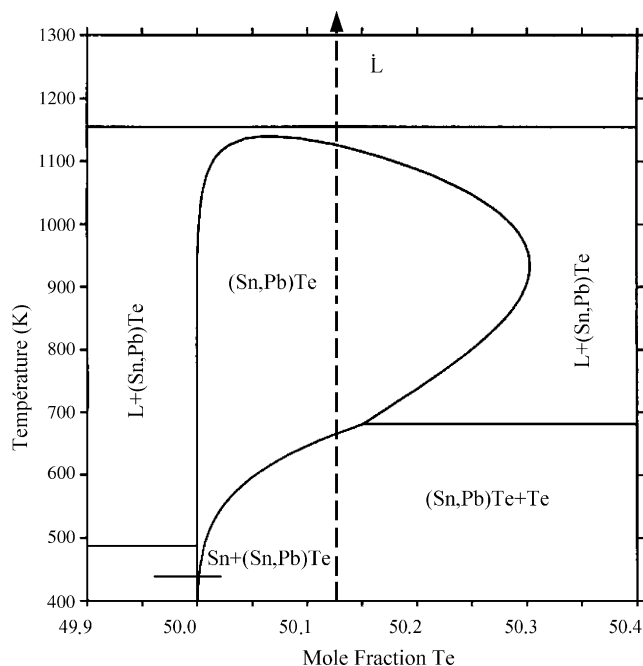


Fig. 6. Enlarged central part of the  $\text{Sn}_{35}\text{Te}_{65}$ -Te section from Kattner's results [18].

assumption. For the sample milled for 31 h, powders keep the same aspect during heating and pure elements are no longer present, then the origin of the exothermic effect must be different in this case. As it was shown from Rietveld refinements [19] for the PbTe MA powders, it could be associated with a relaxation of strains into the material after completion of the reaction.

Since it is an exothermic reaction which originates the PbTe formation in the MA process [15], we could have expected the same mechanism for  $\text{Pb}_{0.65}\text{Sn}_{0.35}\text{Te}$ . Nevertheless, in the latter case, a further reaction should have been observed, indeed formation of SnTe from the elements is also highly exothermic ( $\Delta H_f = -63 \text{ kJ mol}^{-1}$  at 500 K, [20]). Even if this reaction appears when a mixture of lead, tin and tellurium corresponding to the stoichiometry of  $\text{Pb}_{0.65}\text{Sn}_{0.35}\text{Te}$  is heated at 20 K/min (Fig. 7), SnTe has never been observed in MA powders. The mixture seems to behave in a different way because of the presence of a liquid phase, indeed the endothermic effect at 500 K corresponds to the melting of tin. In comparison with a mixture of lead and tellurium heated in the same conditions (Fig. 8), the reaction temperature associated to the formation of PbTe is also lowered by the liquid phase.

#### 4. Conclusion

This study shows that homogeneous  $\text{Pb}_{0.65}\text{Sn}_{0.35}\text{Te}$  can be obtained, from elemental powders by MA in a

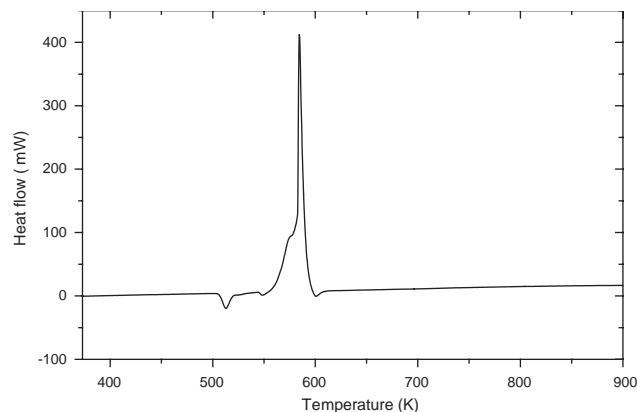


Fig. 7. Thermogram obtained on heating from elemental powders of Pb, Sn, Te.

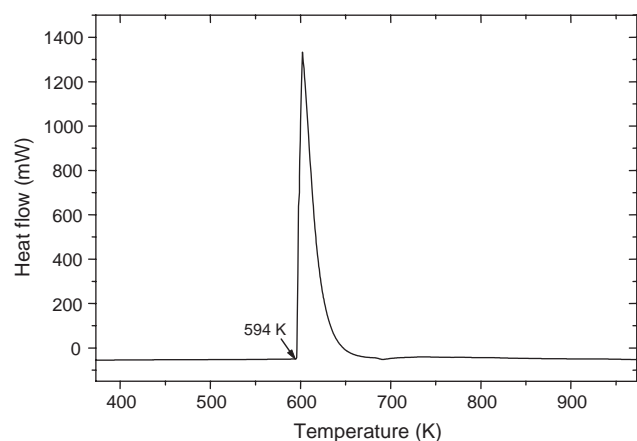


Fig. 8. Thermogram obtained on heating from elemental powders of Pb and Te.

relatively short time, 31 h of milling, at least in the experimental conditions reported here. The systematic analyses performed on the mechanically alloyed powders, using X-ray diffraction (XRD), differential scanning calorimetry (DSC) and scanning electron microscopy (SEM) lead us to conclude, as it was observed for the PbTe MA powders, a mechanism of formation originated from an exothermic reaction. The required time to get a homogeneous phase  $\text{Pb}_{0.65}\text{Sn}_{0.35}\text{Te}$  is longer (31 h) than that needed for PbTe (3 h). This difference might be due to the high resilience of tin. Indeed, even after 12 h of milling; pieces of tin are still  $\sim 1 \text{ mm}$  long. This property might also hinder the reaction between tin and tellurium.

#### Acknowledgments

One of the author (Nathalie Bouad) would like to thank Thalès society for financial support.

## References

- [1] V. Fano, in: D.M. Rowe (Ed.), *CRC Handbook of Thermoelectrics*, CRC Press, Boca Raton, 1995, pp. 257–266.
- [2] D.M. Rowe, C.M. Bandhari, A review of lead telluride technology at Uwist, in: *Proceedings of the Sixth International Conference on Thermoelectric Energy Conversion*, University of Texas, 1986, pp. 43–54.
- [3] J.W. Wagner, R.K. Willardson, *Trans. Metall. Soc. AIME* 242 (1968) 366–371.
- [4] A. Machonis, I.B. Cadoff, *Trans. Metall. Soc. AIME* 230 (1964) 333–339.
- [5] D. Borde, H.J. Albany, M. Roudier, M. Vandevyver, *C. R. Acad. Sci. Paris* 260 (1965) 5235–5238.
- [6] D. Borde, H.J. Albany, M. Vandevyver, *C. R. Acad. Sci. Paris* 262 (1966) 123–126.
- [7] A.R. Calawa, T.C. Harman, M. Finn, P. Youtz, *Trans. Metall. Soc. AIME* 242 (1968) 374–383.
- [8] D.M. Rowe, C.M. Bandhari, *Appl. Phys. Lett.* 47 (3) (1986) 255–257.
- [9] M. Orihashi, Y. Noda, L.D. Chen, T. Goto, T. Hirai, *J. Phys. Chem. Solids* 61 (2000) 919–923.
- [10] A.F. Ioffe, *Semiconductor Thermoelements and Thermoelectric Cooling*, Infosearch, London, 1957.
- [11] K. Hasezaki, M. Nishimura, M. Umata, H. Tsukuda, M. Araoka, in: *Proceedings of the 12th ICT*, 1993, p. 307.
- [12] B.A. Cook, B.J. Beaudry, J.L. Harringa, W.J. Barnett, in: *Proceedings of the Ninth ICT*, 1990, p. 234.
- [13] D.M. Rowe, V.S. Shukla, N. Savvides, *Nature* 290 (1981) 765.
- [14] J. Schilz, M. Riffel, K. Pixius, H.J. Meyer, *Powder Technol.* 105 (1999) 149.
- [15] N. Bouad, R.M. Marin-Ayral, J.C. Tedenac, *J. Alloys Compd.* 297 (2000) 312–318.
- [16] T.F. Tao, C.C. Wang, *Physics of IV–VI Compounds and Alloys*, Gordon and Breach Science Publishers, London, 1974, pp. 15–23.
- [17] D. Bernache-Assolant, *Chimie-physique du frittage*, Hermès, Paris, 1993.
- [18] U. Kattner, H.L. Lukas, G. Petzow, B. Gather, E. Irle, R. Blachnik, *Z. Met. Kd.* 79 (1988) 32–40.
- [19] N. Bouad, L. Chapon, R.M. Marin-Ayral, F. Bourree-Vigneron, J.C. Tedenac, *J. Solid State Chem.* 173 (2003) 189–195.
- [20] I. Barin, *Thermochemical Data of Pure Substances*, VCH, Weinheim, Germany, New York, 1993.